# WEAR OF ELASTOMERIC SEALS IN ABRASIVE SLURRIES

H. M. Ayala, D. P. Hart,

and

O. Yeh, M. C. Boyce

Massachusetts Institute of Technology Department of Mechanical Engineering Cambridge, MA 02139-4307

#### **ABSTRACT**

Seals are a critical aspect of machinery that operates in the presence of abrasive slurries. Seals act to maintain machine lubrication and prevent abrasives from affecting critical components. Over time, however, the slurry will wear the seal and lead to a loss of lubrication and eventual machine failure. It is therefore important to investigate the seal wear process in aims of improving seal design and performance.

The wear process was studied by visualizing and recording the operation of the seal through a window using time-lapse video. Images from the test show that the wear process occurs in two stages: the break-in period and the aggressive wear period. During the break-in period the seal does not wear. During the aggressive wear period, however, particles under the contact band cluster and form an abrasive front that erodes the seal lip at a rapid rate.

Based on these observations, the seal geometry was changed to include the periodic placement of various texture topologies, including (1) a depression surrounded by a protrusion, (2) a protrusion only and (3) a depression only. Textures featuring protrusions act to extend the break-in period and decrease the wear rate of the aggressive wear period. Seals with the protrusions-only texture outlived non-textured seals by a factor of eight.

#### 1. INTRODUCTION

Seal manufacturing is a \$2 billion a year industry in the United States, but the cost in terms of loss of productivity and equipment resulting from poor seal performance is far greater [1]. Seals are critical components in virtually all mechanical devices. Devices containing hundreds of seals are common and the failure of a single seal often has catastrophic consequences. Accordingly, tremendous effort has gone into improving seal design. Despite this effort, progress has been slow and seals today appear, for the most part, identical to seals used thirty years ago. Nonetheless, there has been significant progress in seal technology in terms of both operational life and sealing characteristics. Much of this improvement has been the result of empirical, trial-and-error engineering. The complexity of seals and the difficulties associated with resolving essential parameters, both material and geometric, have hindered the effectiveness of experimental and theoretical approaches to seal design. There have, however, been a number of significant fundamental studies that have improved our understanding of seals and of how they fail. In 1967, Hirabayashi, et al. [2] optimized the seals used in the cooling system of automobiles after studying how salt used in the anti-freeze crystallized and damaged the seal. They showed that seals made from harder materials resisted abrasion better at low contact pressures, whereas softer materials performed better at higher loads. Later, Golubiev and Gordeev [3] improved the seal design of water pumps operating in fluids

with high concentrations of abrasive particles. More recently, Bratthäll [4] modified the design of pumps operating in abrasive and clogging media to improve their reliability. In both cases, the new designs incorporated the use of abrasion-resistant materials, changes to the sealing geometry, and changes to the seal loading mechanism.

This paper presents an experimental and numerical investigation of the wear process of a face seal operating in an abrasive slurry. The fundamental process by which particles are entrained into the seal surface is illustrated through a sequence of images using time-lapse photography and a method of averting this particle entrainment is presented along with numerical and experimental data quantifying its effectiveness. By correlating wear rate and particle entrainment behavior with changes in seal geometry, the basic mechanics governing abrasive wear are postulated and tested. This theory is supported with quantified measurements of lubricant film thickness using laser-induced fluorescence (LIF), finite element modeling of each seal under load quantifying the seal/bushing contact pressure distribution, and testing of the wear behavior of each seal.

#### 2. EXPERIMENTAL SETUP

# Seal Assembly

The seals tested in this research belong to the general class referred to as face seals. A face seal differs from the more common shaft seal in that it contacts its bearing surface along a plane rather than along the perimeter of a shaft.

As shown in Figure 1, the prototypical face seal consists of a wedge-shaped seal lip manufactured from an elastomeric compound. It contacts a moving part (i.e., the bushing) to provide sealing action. The width of the seal is taken to be the distance over which the seal can make contact (indicated in Figure 1 as 4.82 mm). The diameter of the seal tested is 84 mm.

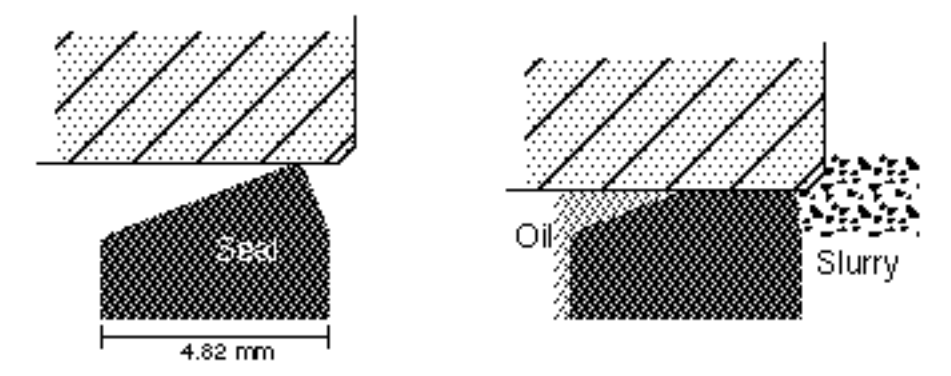
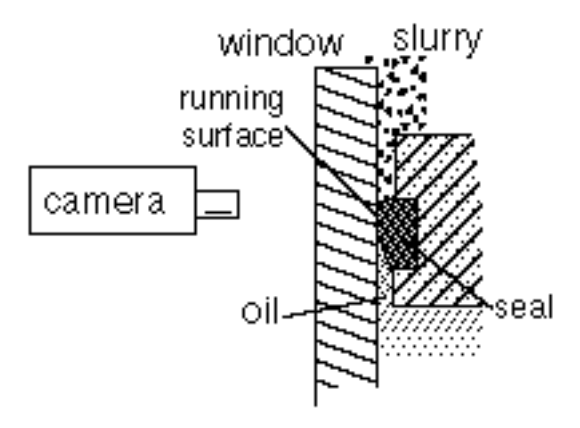


Figure 1: A cross-section view of the seals tested in this paper. The left image shows the seal with no load applied. On the right, the seal has been compressed to its operating load.

The operating conditions of the seal are such that: (1) the seal assembly is axially compressed in order to establish a high contact pressure between the seal lip and the bushing, (2) the seal lip and the bushing displace in a slow oscillatory motion with respect to each other, and (3) the seal lip is surrounded by an abrasive slurry.



*Figure* 2: The setup used for testing the seals. A CCD camera captures the wear process by focusing on a seal operating against a glass window.

# Visualization Setup

Figure 2 shows the setup used for observing the operation of the seals. A seal is installed in a mount and pressed against a glass window. A 4-bar linkage connected to an electric motor oscillates the mount and seal back and forth sinusoidally through a 30-degree arc.

During the tests, a seal of 84 mm in diameter was compressed to 2.2 kN and oscillated at a speed of 60 cycles per minute. One cycle is taken as the movement of the seal from one end position to the other. In this manner, two cycles are required to return the seal to its original position. This average contact pressure was 8 MPa and the maximum sliding speed was 34.56 mm/s. The abrasive slurry in which the seal was operated was composed of a mixture of fireclay, bank sand, and water.

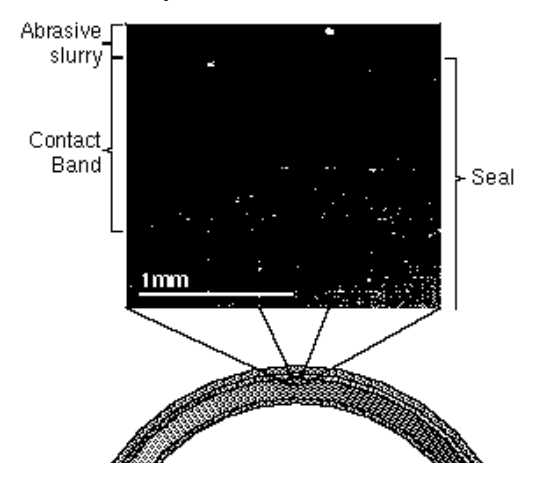


**Figure 3:** Schematic of seal showing region imaged by the CCD camera. A typical image captured by the CCD camera is shown with labels of the observable salient features.

To observe the wear process, a CCD camera was focused on the edge of the seal through the window. Images from the camera and information from a position encoder were transferred to a computer through a video capture board and digitally recorded. The 520 by 460 pixel images correspond to an area on the seal edge measuring 2.05 mm by 1.81 mm, Figure 3. In the image, the abrasive slurry appears as a white substance near the top.

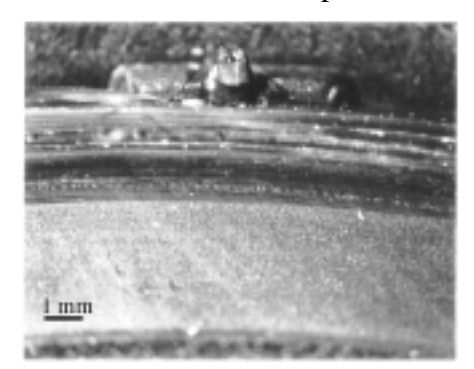
### Laser Induced Florescence Setup

Laser Induced Florescence (LIF) was used to visualize lubricant film thickness. This technique involved using a laser to fluoresce dye that has been dissolved in the oil. A low-pass filter is used to isolate the fluorescence of the dye from the background laser light, thus enabling the concentration of dye and hence oil to be measured [6].

The oil was dyed using Rhodamine 6-G dissolved in a dichloromethanol. The dichloromethanol uniformly distributed the dye in the oil. The solvent was then allowed to evaporate, minimizing its effect on lubrication. Dye concentration was adjusted to provide linear florescence intensity in the film thickness range observed. A 1-watt argonion laser was used as the source of illumination and an 8-bit Pulnix TN9701 520 by 460 pixel CCD camera equipped with a low-pass 550nm filter recorded the dye florescence intensity. In all cases presented here, LIF images of the seal were taken while the seal was loaded to operating conditions but in the absence of the abrasive slurry.

#### 3. FINITE ELEMENT MODELLING

Experimental measurements of seal wear clearly demonstrate that the abrasive slurry greatly accelerates wear. In the absence of this slurry, the seal tested showed practically no signs of wear. Visual inspection of worn seals shows that particle abrasion is responsible for the increase in wear rate (see Figure 4). This abrasion occurs from repeated traversing of the seal under axial compression in the presence of trapped particles. The particles induce a locally high tensile stress in the elastomer which, in turn, contributes to the abrasive wear of the elastomer. As will be discussed later in the paper, the magnitude and distribution in the contact pressure at the interface between the seal and the bushing can impede the ingression of particles. Therefore, the nature of this interfacial contact pressure is a critical aspect to effective seal performance and wear. To obtain an accurate understanding of the contact pressure distribution for both non-textured and textured seals, finite element analyses of the seal system under load were conducted. Details regarding specifics of the finite element models are given in the appendix. The results of primary interest are the distributions in seal-bushing contact pressure of each seal and are presented in subsequent sections.



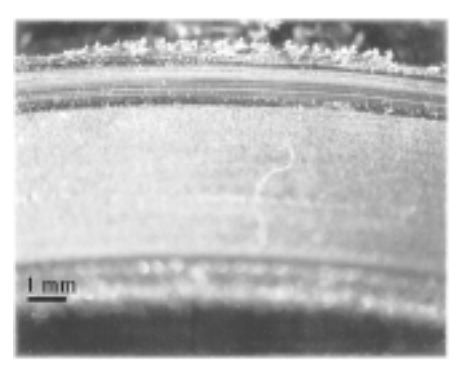


**Figure 4:** The lip of two seals worn against steel (left) and glass (right) in the presence of an abrasive slurry. The wear tracks on the surface of the seal are characterized by a smooth surface in the interior, and a grooved surface on the outside. The smooth surface is typical of wear produced by small particles, whereas the grooved surface is typical or larger particles [5].

#### 4. SEAL PERFORMANCE RESULTS

One of the difficulties in investigating seal performance is the operation time required to achieve failure or, at the least, to achieve noticeable wear on the seal surfaces. Because of this, statistically meaningful tests are nearly impossible on a laboratory scale. In addition, the concept of seal failure is ambiguous in that acceptable leakage rates depend on the application.

In the current study, rather than define performance in terms of leakage per unit time as is typically done, we have instead quantified the wear rate in terms of portion of the seal lip contact surface worn per number of oscillation cycles. This is easily accomplished as the abrasive slurry wears the seal lip progressively from the outside to the inside. Defining wear rate in this manner provides an unambiguous means of comparing seal performance. In addition, by operating the seals against a glass bearing surface, the wear rate per cycle can be quantified without removing the seals from the test facility and without disturbing surface contact features that form between the seal lip and the bearing surface during operation. This method of testing seals provides an unobtrusive means of observing particle entrainment between the seal lip and the bearing surface allowing key contact features to be observed in real time as the wear rate is quantified.

The wear rate of a seal against a glass bearing surface was found to be significantly greater than the rate against a steel bearing surface. The observed characteristic wear patterns on the surface of a seal tested against glass were, however, comparable to those tested against steel. Measured trends in seal wear rate were found to be similar for both seals tested against glass bearing surfaces and seals tested against steel bearing surfaces. It is believed that a secondary wear mechanism is responsible for the increase in wear of a seal against glass bearing surfaces. This wear mechanism appears to be the result of the abrasive slurry grinding at the glass bearing leaving a roughened surface that, by itself, erodes the seal lip. As will be discussed herein, the primary mechanism of wear in which particles are entrained under the seal lip and wear the surface is believed to be identical for wear of seals against glass and steel. Thus, seal tests against glass not only allow the wear process to be observed and quantified, it allows accelerated testing of seals providing significantly more data and allowing more design comparisons to be made than would otherwise be possible.

Both non-textured and textured seals are thus studied via testing against glass. Below, results are presented first for the non-textured seal and then for the textured seals showing the visualization data, the LIF data, and the finite element analysis.

#### 4.1 NON-TEXTURED SEAL

The geometry of the non-textured seal was shown earlier in Figure 1. The seal is now loaded and tested against glass as described in Section 2. The distribution in contact pressure under a static axial load as calculated by finite element analysis is shown in Figure 5. We note that the seal lip geometry is designed to provide a high edge contact pressure in an attempt to prevent the entrainment of particles. This high edge contact pressure decreases towards the inside of the seal facilitating lubrication of the seal/bushing interface. The LIF results for this same loading are shown in Figure 6 and indeed show the oil film thickness mimics the seal/bushing interface pressure of Figure 5. Namely, where the oil film decreases, the interface pressure increases. This particular seal lip geometry seems to provide an ideal compromise for satisfying the requirements of providing lubrication while preventing particle penetration.

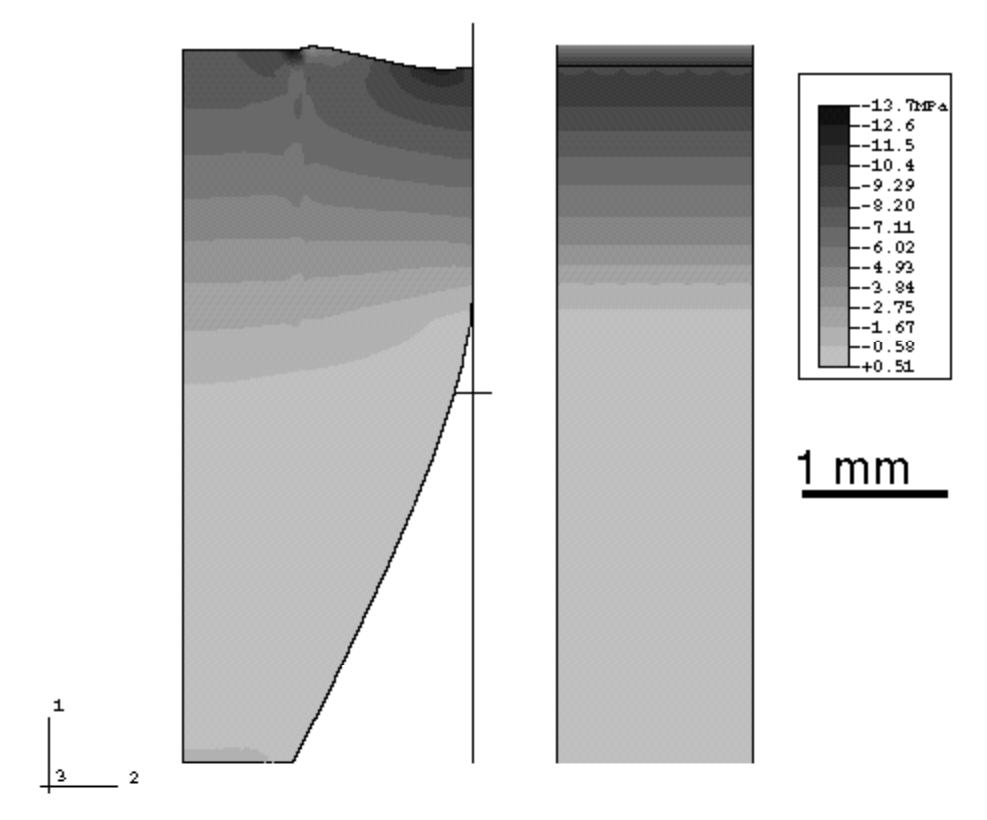


**Figure** 5: A finite element model of the seal lip showing the seal/bearing contact pressure distribution $^{\dagger}$ . A comparison of this model and the LIF image of the seal shows that oil film thickness is smallest at the point of highest contact pressure. The line shows the area of detail presented in Figure 6.

During operation, the visualization setup described in Section 2 monitors the penetration of particles into the contact band as a function of cycles of operation. Images from the visualization test reveal negligible penetration of the particle front until seven thousand cycles of operation. After seven thousand cycles, particles from the abrasive slurry penetrate the contact band quickly. In their tests of water pump seals, Golubiev and Gordeev [3] observed the same pattern of a long period of little or no wear preceding an aggressive wear period. They named the two stages the *break-in* period and the *aggressive wear* period.

 $<sup>^{\</sup>dagger}$  Here, contours of the strain component  $_{33}$  are shown. Where the lip is in contact with the bushing,  $_{33}$  is eqivalent to the contact pressure and it is compressive.

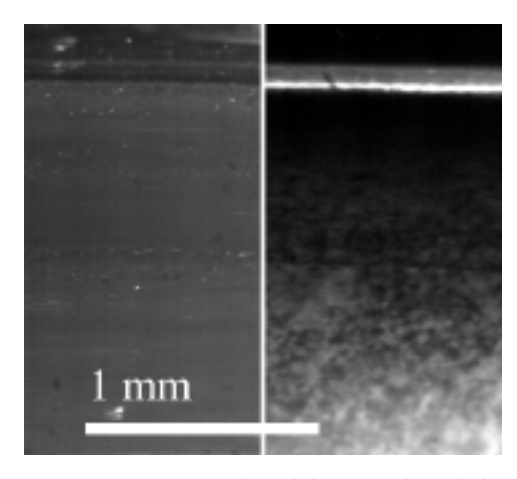
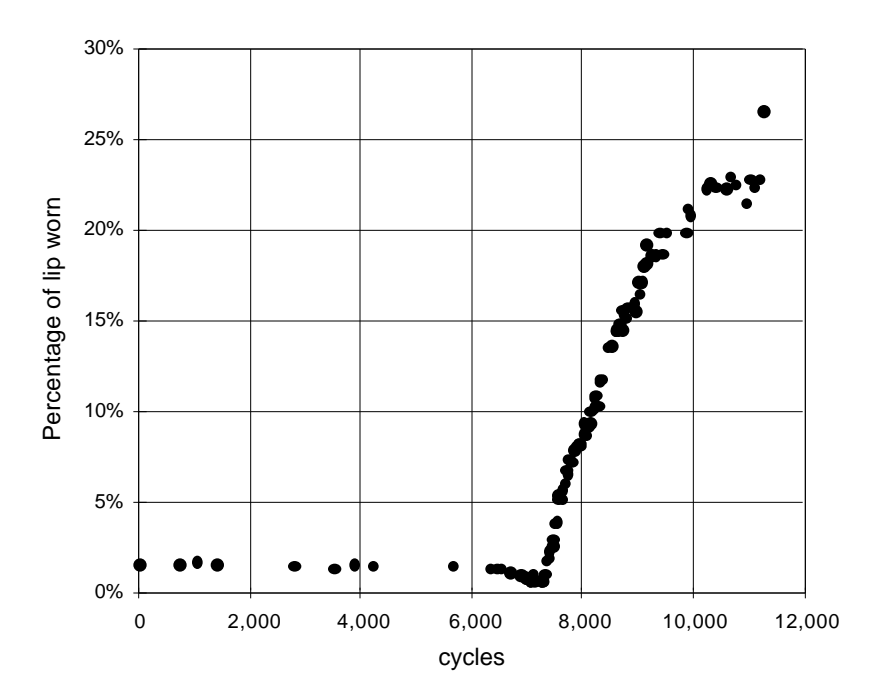


Figure 6: Two views of an non-textured seal lip, in white light (left) and by means of laser-induced fluorescence (right). By dying the seal lubricant with Rhodamine 6G and illuminating the seal with an argon laser, the oil film thickness under the seal lip can be quantified from the dye florescence intensity. A calibration relating the light intensity to the oil film thickness was not performed.



**Figure** 7: The penetration of particles into the contact band of the seal as a function of cycles of operation. Seal wear is measured as the percentage of the seal lip that the abrasive slurry has penetrated. Note that there are two distinct regions of operation. The break-in period of wear is characterized by a very low wear rate and can be seen as the region from 0 to 7,000 cycles of operation. The aggressive wear period occurs after 7,000 cycles of operation.

A plot showing the advance of particles as a function of cycles is shown in Figure 7. It clearly delineates a break-in period and an aggressive wear period. A summary of images taken during the aggressive wear period (between seven and ten thousand cycles) is shown in Figure 8. Wear of the seal lip is a direct consequence of the penetration of the particle front. As Figure 7 shows, once a particle front is established, penetration (and thus wear) proceeds rapidly. Within the worn region of the seal lip, particles are

observed to cluster into periodic radially aligned bands (see Figure 9). These bands are believed to be responsible for the transition from the break-in period to the aggressive wear period. The accumulation of particles within these bands presses against the seal lip locally reducing the seal lip/bearing contact pressure allowing larger particles to penetrate under the lip surface (see Figure 10). Wear of the seal lip then results from direct abrasion by particles and abrasion due to particle damage of the bearing surface. Thus, once these particle bands form, wear proceeds rapidly.

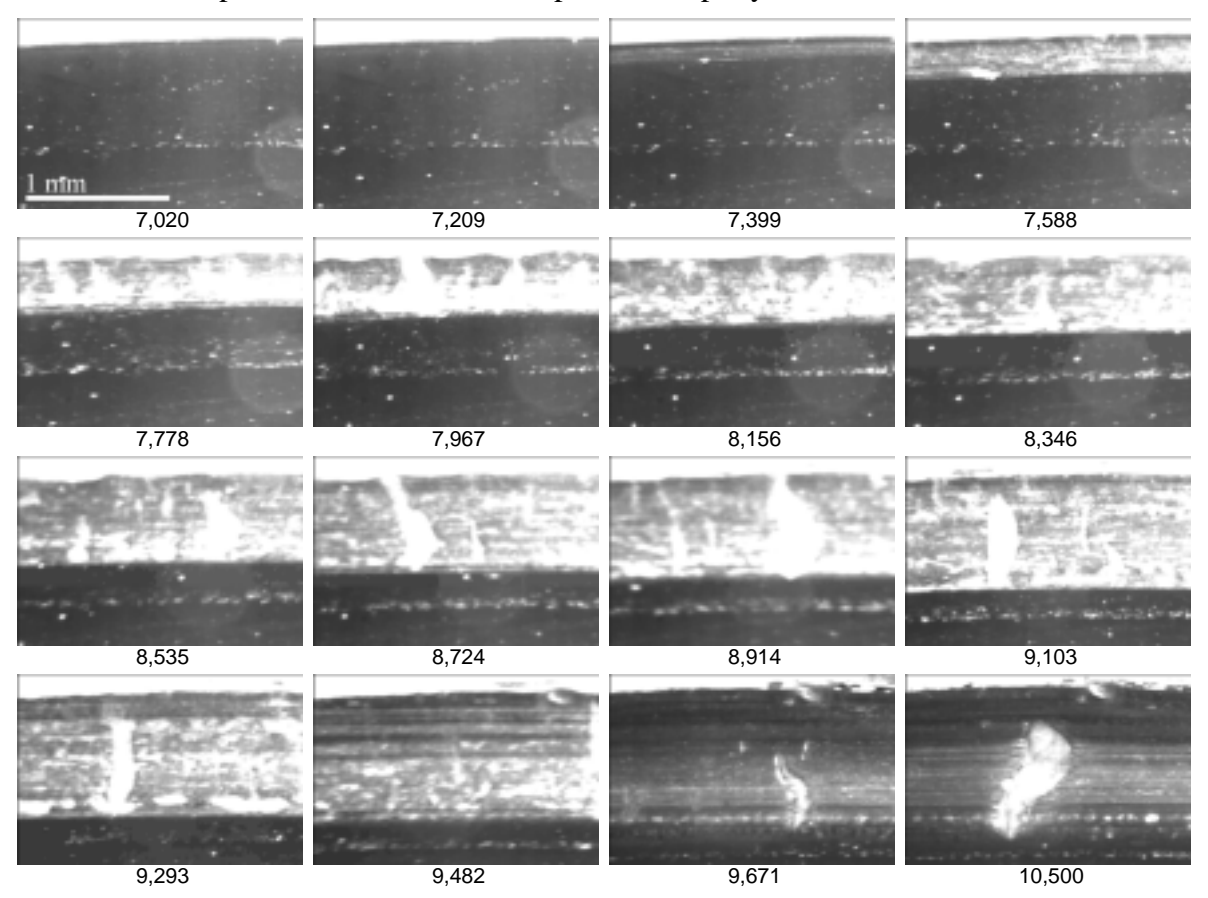


**Figure** 8: A sequence of pictures showing the advance of abrasive particles into the contact band during the aggressive wear period. The number of cycles that the seal had been operated is shown below each picture. Note the radial clusters of particles that form under the seal lip observable from 8,000 cycles of operation on. These clusters are believed to advance the particle front by forcing the seal lip away from the bearing surface thereby causing the aggressive wear period.

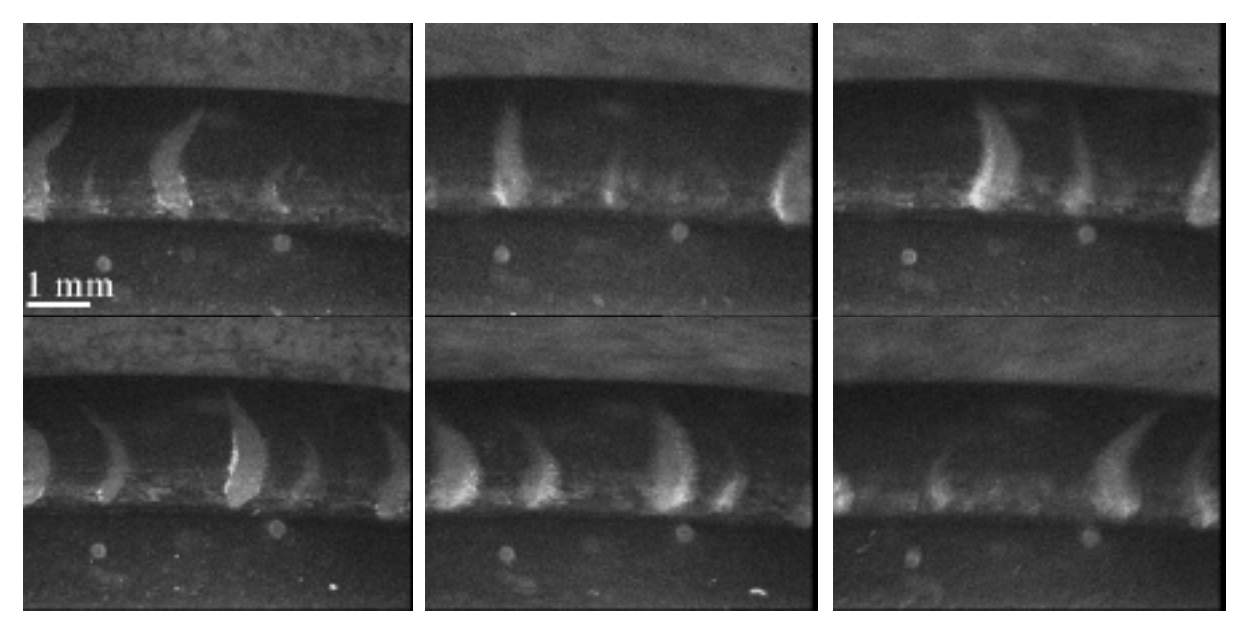


*Figure 9*: An image sequence showing the motion of particles trapped in the seal contact band. These particles cluster into radially aligned tear-shaped formations.

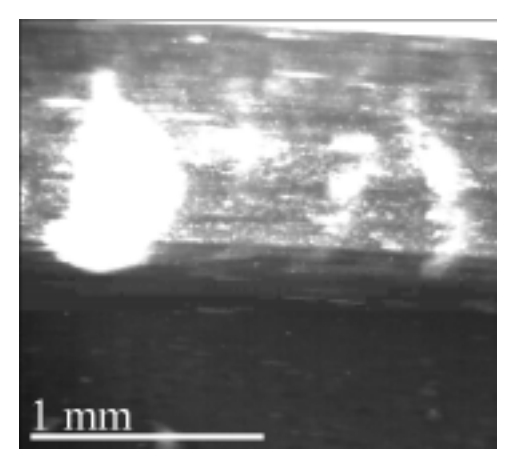


*Figure* 10: The round end of a particle cluster is seen penetrating the seal contact band. This is believed to be the process by which aggressive wear occurs.

#### 4.2 TEXTURED SEALS

Visualizing the wear process suggests that the life of the seal can be extended in two ways. The first is to prevent the initial formation of the particle front. The second is to prevent the propagation of the particle front once it has penetrated the contact band.

In an effort to retard the progression of the particle front, three textured seal designs were conceived: a circular bump-and-hole combination, tangential slits, and radial slits, Figure 11. The designs were based on the hypothesis that the textures would act as a trap for particles, a mechanism analogous to situations in which surface features are added to contain wear debris [7]. As will be shown, the textured seal design is extremely effective, but the mechanism is in fact radically different. Each of the three texture designs was cut into one quadrant of a seal leaving one quadrant unmodified. The tangential slits were cut to a length of 2 mm and spaced 1 mm apart in the radial direction. The radial slits were cut to a length of 1.5 mm and spaced 2.5 mm apart. The

holes had a diameter of 0.3 mm and were space 2.5 mm apart. The seal was then operated against a glass bushing in an abrasive slurry for 10,000 cycles. As can be seen in Figure 11, all of the texture patterns significantly reduced the rate of wear. The bump-and-hole combination, however, proved to be the most effective.

To further determine what aspect of the bump-and-hole texture produced the reduction in wear, seals with bump-only, hole-only, and bump-and-hole were molded, Figure 12. The diameter of the bump was 1 mm, and the diameter of the hole 0.5 mm. The features were placed evenly around the seal perimeter at a spacing of approximately 2.5 mm. As shown in Figure 13, the bump-and-hole textured seal exhibits a break-in period more than twice as long as the non-textured seal (16,000 instead of 7,000 cycles), and a wear rate five times smaller than a non-textured seal (0.05 rather than .25 mm per thousand cycles). Although texturing was found to successfully increase seal life, the texture was *not* found to act as a trap for abrasive particles as evident in the images of Figure 14.

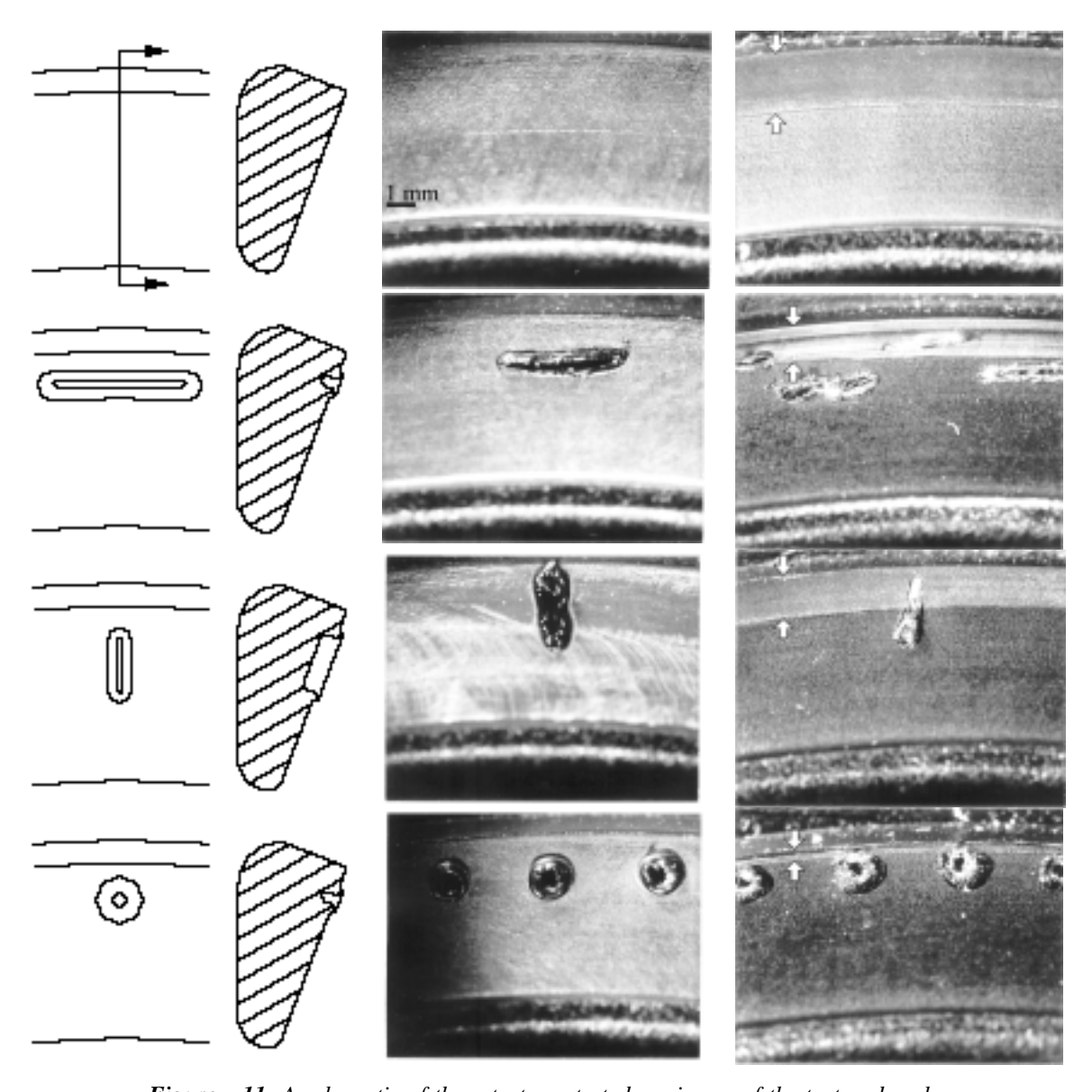


Figure 11: A schematic of three textures tested, an image of the textured seals, and the resulting observed wear (indicated by arrows). All of the tested textures resulted in reduced wear rates but the bump-and-hole texture (bottom) was superior to the tangential slits (2nd from top) and radial slits (3rd from top). The seal containing these textures was oscillated approximately 10,000 cycles.

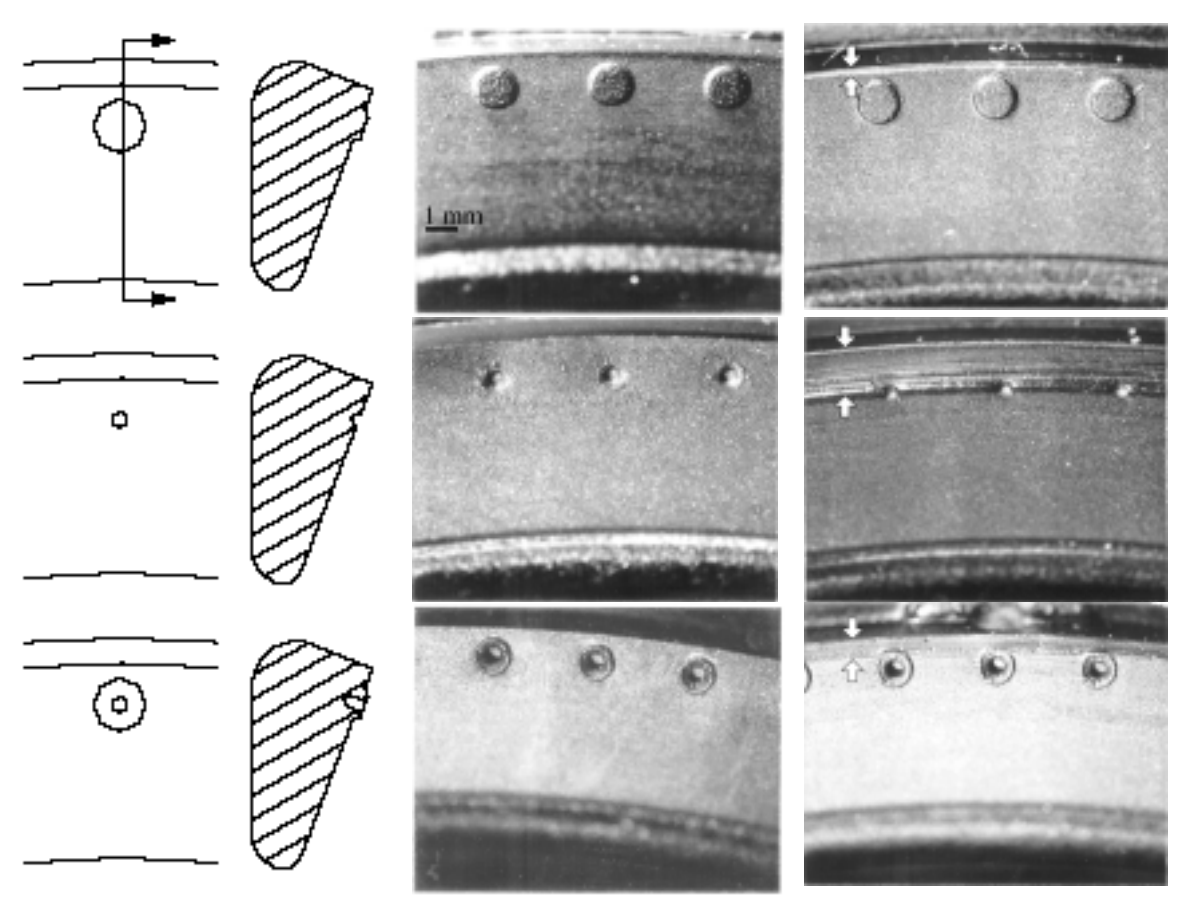


Figure 12: A schematic of three textured seals, an image of the unworn tested seals, and the resulting observed wear. The bump-only pattern (top) proved far superior to the other texture geometries in reducing the seal wear rate (see Figure 15). For the seals shown the operating times were, 57,000 (bump-only), 10,000 (hole-only), and 35,000 cycles (bump-and-hole).

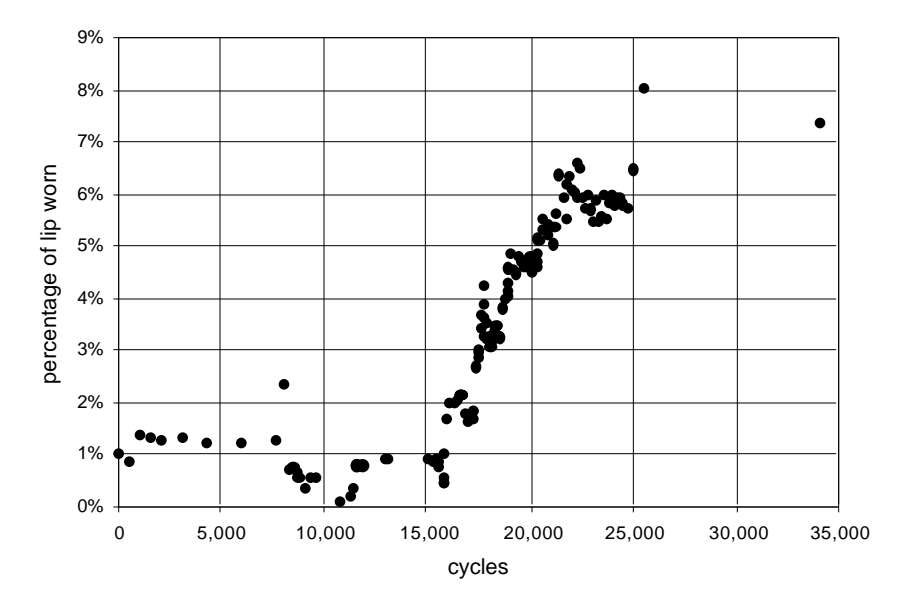


Figure 13: The penetration of particles into the contact band of the bump-and-hole textured seal as a function of cycles of operation. The penetration of particles is plotted as the distance of penetration divided by the width of the seal lip. The aggressive wear period begins at 15,000 cycles of operation. This is more than double the number of cycles observed in non-textured seals (Figure 7). During this operational period, the wear rate is less than 1/5th of that occurring in non-textured seals.

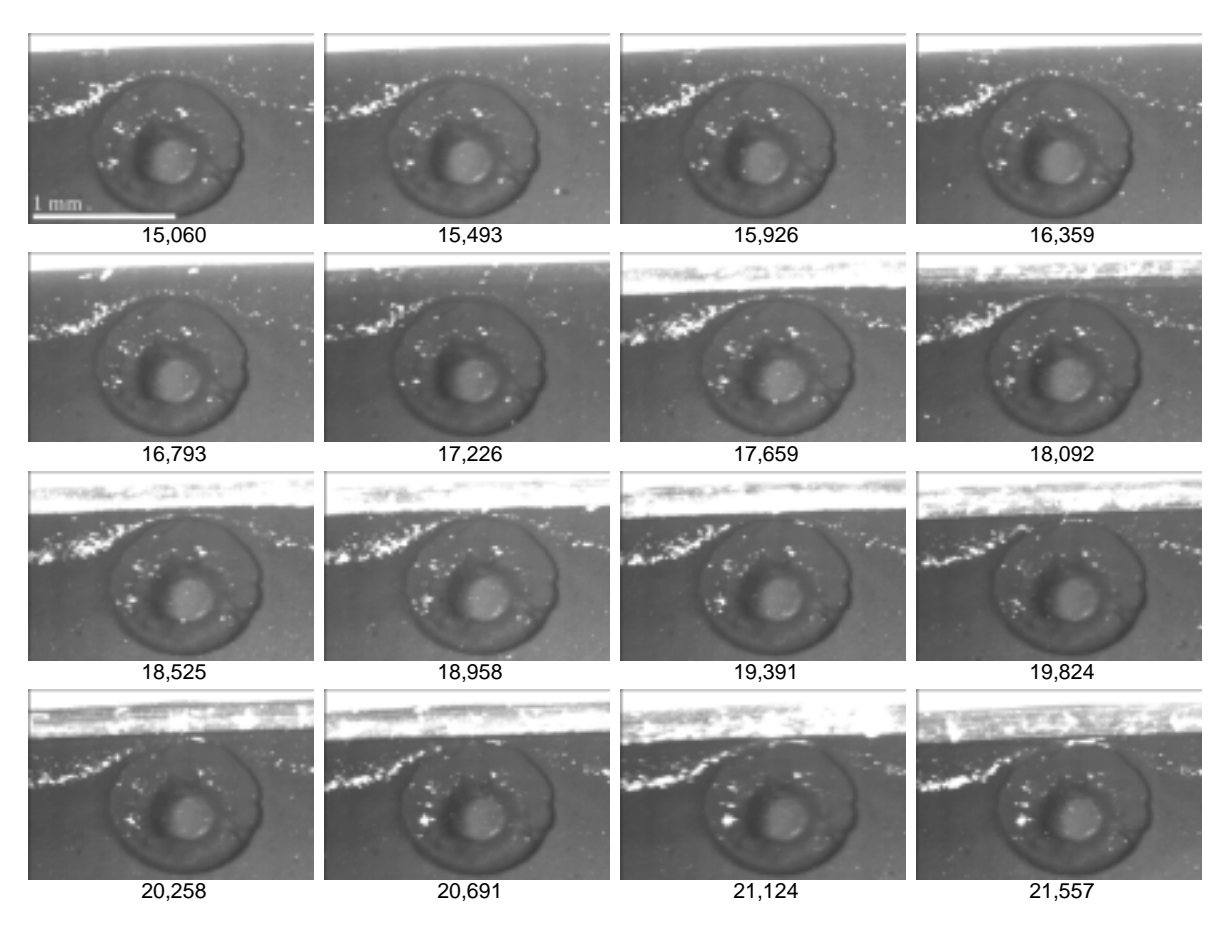


Figure 14: A sequence of pictures showing the advance of abrasive particles into the contact band of a seal textured with a bump-and-hole texture. The number under each frame corresponds to the number of cycles of operation. Note how the seal contact band swerves around the texture feature. During the aggressive, wear period, after 15,000 cycles of operation, radial particle clusters can be seen forming in the region between the texture feature and the outside edge of the seal. Eventually, the particle front abrades through the texture feature but at a much reduced rate compared with non-textured seal wear rates.

Interestingly, of the three texture topologies studied, only those that contained a protrusion (bump) acted to significantly reduce the wear rate; the hole-only topology showed no significant change in wear. Plots of particle front vs. oscillations for the various seals are superposed in Figure 15.

In order to further understand how texturing reduces wear, the effects of texture on the contact pressure and lubricant distribution were studied by means of finite element analysis and laser-induced fluorescence (LIF). In the examination of the non-textured seal behavior, the correlation between the seal/bushing interface pressure and the thickness of the oil film between the seal and the bushing was shown in Figure 6 and Figure 5. Similarly, by comparing the LIF image of the bump-and-hole texture seal shown in Figure 16 with the finite element model of the same texture topology as shown in Figure 17, one can see that the areas of lowest lubrication correspond to the areas of highest contact pressure.

The texture thus acts to provide an alternating pattern of low contact pressure regions immediately adjacent to high contact regions. The regions of high contact pressure act as

barriers to particle penetration whereas the low-pressure regions facilitate the lubrication of the high-pressure regions.

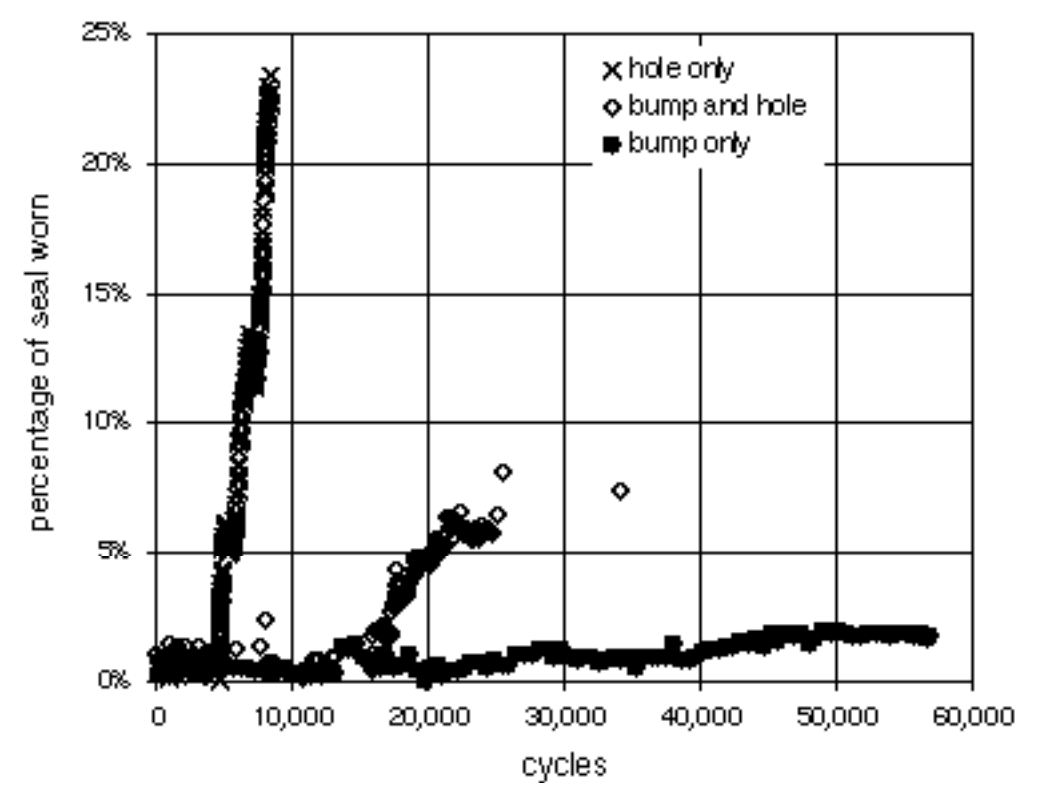


**Figure 15:** A comparison of the wear rate measured for the three texture patterns shown in Figure 12. The bump-only texture pattern exhibits far lower wear rates than the hole-only and bump-and-hole combination texture patterns. Even after 60,000 cycles of operation, the seal with bump-only texture shows no sign of entering the aggressive wear period.

The contact band of the bump-and-hole texture combination, shown in Figure 17, swerves around each of the texture cells instead of running parallel to the edge of the seal as in the non-textured seal. The low-pressure regions around the bump-and-hole texture provide a means by which oil can be transported by capillary action into the seal/bearing contact region. This increased lubrication prevents the adjacent high contact pressure regions from quickly abrading against the bearing surface. The bump-and-hole texture thus provides a means of increasing contact pressure while, at the same time, increasing lubrication. The points of highest contact pressure are as crucial in retarding wear as increased lubrication. In video images taken during wear tests, the outer edge of the rim is seen breaking up clusters of particles that accumulate inside the contact band. Like the bump-and-hole combination, the bump-only texture acts to provide regions of low contact pressure adjacent to regions of high contact pressure as shown in the finite element contour of contact pressure in Figure 18. The bump-only texture contact pressure profile is similar to that of the bump-and-hole combination, Figure 17 and Figure 18. The wear rate of the bump-only seal, however, is lower than the bump-andhole, Figure 15. The hole-only texture profile has a lower peak contact pressure profile (Figure 19) and exhibits a corresponding increase in wear rate.

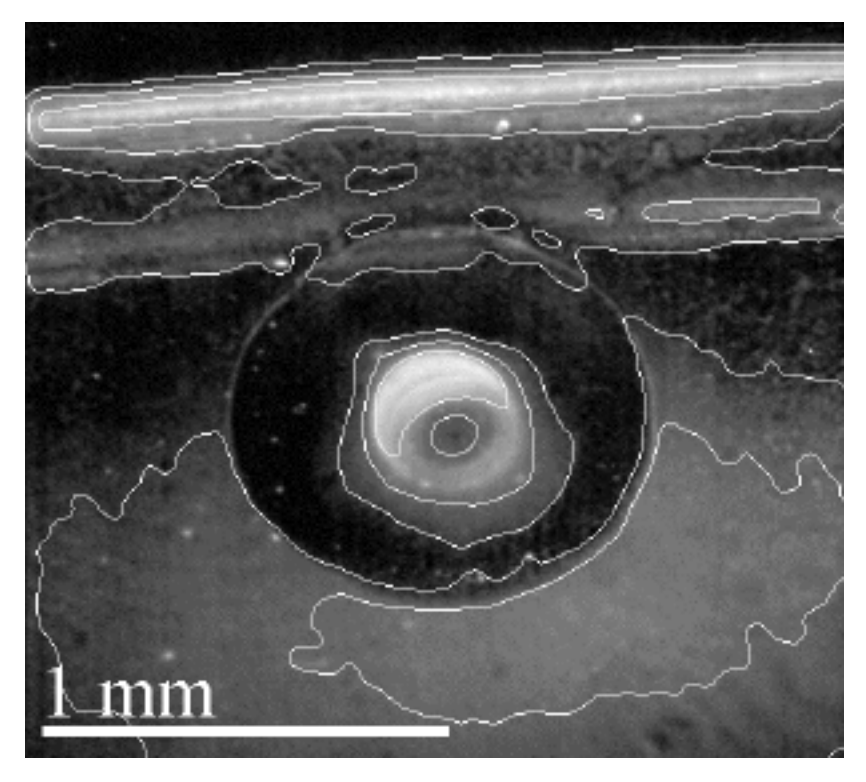


Figure 16: The lubrication of a bump-and-hole combination textured seal as revealed by laser-induced fluorescence. Oil film thickness is indicated qualitatively by light intensity in this figure. Increased lubrication thickness can be observed in the center of the textured feature and in the low contact pressure region around the outside edge of the textured feature. The bright region along the outside edge of the seal is a meniscus of oil that clings to this region by surface tension.

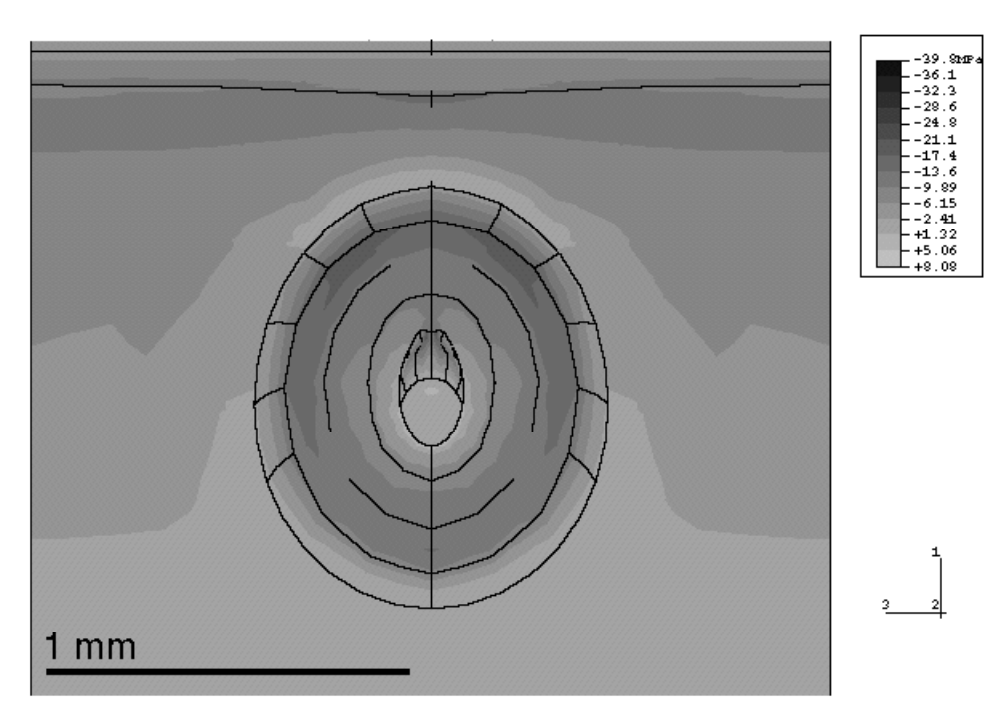
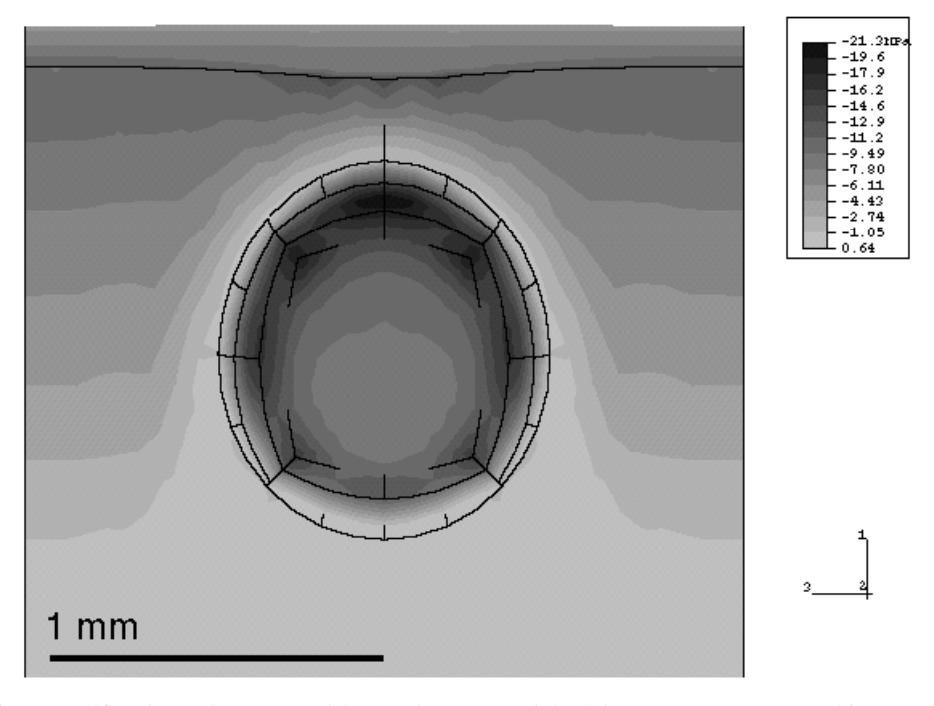
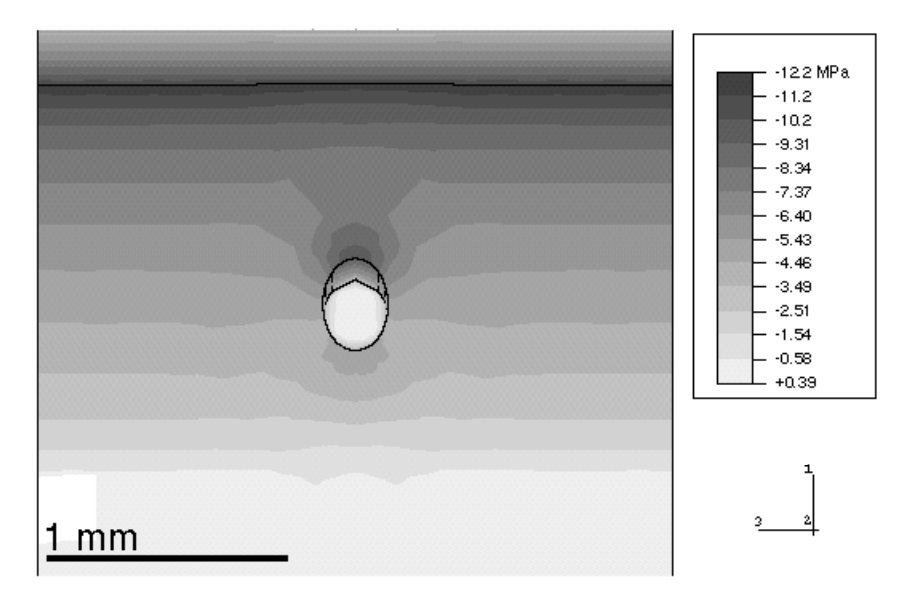


Figure 17: Three-dimensional finite element model of the contact pressure of bump-and-hole texture feature. Note the similarity with the LIF measurements in Figure 16. Areas of low contact pressure collect lubricant redistributing it to adjacent high contact regions during seal operation.



**Figure** 18: Three-dimensional finite element model of the contact pressure of bump-only texture feature. The region of low contact pressure toward the inside of the seal lip and around the texture feature is far greater than around the bump-and-hole texture feature shown in Figure 17.



**Figure 19:** Three-dimensional finite element model of the contact pressure of a hole-only texture feature. Near the hole, there is a slight increase in contact pressure. The hole provides a region where lubricant can collect and redistribute during operation but, unlike the bump type texture features, the hole-only feature does not exhibit high contact pressure along the sliding path of the seal next to a well lubricated area. As expected, this textured feature did not function as well as the bump type features.

#### 5. SUMMARY

This paper reports on a study of the wear process of a class of elastomeric face seals which operate in an abrasive slurry under slow oscillatory motion. The basic function of the seal is to prevent leakage of lubricant. Leakage occurs after a period of operation due to the wear of the elastomeric seal. Therefore, understanding and controlling the principal factors which govern the wear process is critical to the overall life cycle of the entire component.

The wear process was visualized by testing seals against a glass surface; the seals were surrounded by an abrasive slurry. A CCD camera focused on the edge of the seal through the glass and recorded a time-lapse video of the wear process. The wear process was observed to proceed in two stages. In the first stage, termed the break-in period, the seal does not wear. In the second stage, termed the aggressive wear period, images from the tests show that particles from the slurry penetrate the seal radially inward in the form of a front which steadily erodes material from the seal lip.

Clearly, in order to extend the life of the seal, the penetration of particles and the subsequent formation of a particle front should be prevented. Therefore, the seal surface was re-designed to include a periodic placement of texture. Various texture topologies were examined including depressions ("holes"), protrusions ("bumps") and a combination of the two ("hole-and-bump"). Textured seals featuring protrusions were found to significantly lengthen the break-in period of the wear process as well as decrease the wear rate of the aggressive wear period. While the experiments in this paper were performed against a glass bearing surface, tests against a steel bushing verified that texturing also provided longer life under field conditions.

Observations made from the wear videos show that the protrusions, or raised portions, of the texture pattern retard wear by breaking and dissipating particle clusters trapped in the contact band. Finite element simulations show the textured features to provide locally high contact pressures which facilitate the observed break-up of particle clustering. The simulations also show the locally high contact pressure regions to be surrounded by low contact pressure regions. The low contact pressure regions provide neighboring zones of lubrication which act to lubricate the high contact pressure regions and thus prevent their premature wear. The presence of the lubrication zones was verified using laser-induced fluorescence.

In summary, wear of the seal begins once abrasive particles penetrate the contact zone and then proceed to form an abrasive particle front. The new textured seal design facilitates a dramatic extension in the life of the seal by providing locally high contact pressure regions near the seal edge (which act as barriers to particle penetration and clustering) surrounded by low contact pressure regions (which facilitate lubrication of the high contact pressure regions near the seal edge).

# Appendix A: Finite Element Models of Contact Pressure Distribution in Non-Textured and Textured Seals

This appendix describes the finite element models that were used to examine the contact pressure distribution between the seal and the bushing. Non-textured and textured seals were modeled under conditions of axial compressive loading. The commercial finite element code ABAQUS was used in all simulations.

#### A.1 Non-Textured Seal

A face seal design typically consists of an assembly of units which ultimately provide transfer of the load to the seal lip to enable effective contact between the seal lip and the bushing. Since it is the seal lip/bushing interaction which provides the seal, it is this region that we isolate for finite element analysis.

# A.1.1 Geometric Model and Loading Conditions

The non-textured seal possesses axisymmetric geometric and loading conditions. Thus, to utilize the symmetry and reduce the computational complexity of the model, twodimensional quadratic 8-node axisymmetric elements were used. Additionally hybrid formulation elements were used because the seal material is an During operation, telastomer which exhibits nearly incompressible behavior.

During operation, the entire seal assembly is compressed axially. Thus, an axial load is transmitted to the seal lip. However, the seal assembly also acts to constrain the radial displacement of the top surface as well as portions of the inner and outer lateral surfaces. These two loading conditions are simulated by displacement boundary conditions on the appropriate nodes: the top surface of the seal lip is displaced axially until reaching a specified face seal load while nodes along the top surface and portions of the lateral surfaces are constrained from radial displacements.

#### A.1.2 Material Models

Since the seal lip is made of an elastomeric material, the Arruda-Boyce 8-chain model of rubber elasticity was used to model its stress-strain behavior. The Arruda-Boyce model was developed from statistical mechanics and is detailed in Arruda and Boyce [8]. From this model, the following stress-stretch relationship can be written.

$$_{1}$$
 -  $_{2}$  =  $C_{R}\sqrt{N}$  Langevin<sup>-1</sup>  $\frac{chain}{\sqrt{N}}$   $\frac{\begin{pmatrix} 2 - 2 \\ 1 - 2 \end{pmatrix}}{chain}$ 

 ${}_{1}-{}_{2}=C_{R}\sqrt{N}\ Langevin^{-1}\ \frac{{}_{chain}}{\sqrt{N}}\ \frac{\left(\begin{array}{c} 2\\1-\frac{2}{2}\end{array}\right)}{{}_{chain}}$  The constitutive model contains two material properties:  $C_{R}$  and N. The material was modeled using  $C_{R}$  equal to 6.45 MPa and N equal to 7.5. The deformed mesh of a seal lip that has been subjected to an axial appropriate 1 of 2.21 N in the first search of the searc that has been subjected to an axial compressive load of 2.2 kN is shown in figure A.1.

#### A.2 Textured Seals

#### A.2.1 Geometric Model and Loading Conditions

The sealtexturing of the seal surface removes the axisymmetry of the problem and introduces a periodic symmetry. Because of this, a three dimensional model was necessary to model the textured seals. To reduce the size and complexity of the simulation, only a portion of the seal lip was modeled as shown in Figure A.2. The wedge contains one-half a texture cell and is based on a texture spacing of approximately 2.5 mm.

The mesh was constructed from 20 node hybrid brick elements. Displacement boundary conditions restrict the mesh borders from deforming in the 3-direction modeling the periodicity of the cells. Additionally, the non-angled portion of the wedge is restricted from displacing in the 1-direction in order to model the effect of the seal assembly on the seal lip. Loading is accomplished through displacement boundary conditions that deform the wedge against a rigid surface until the appropriate face load has been achieved. Figures A.3, and A.4 show detailed views of the bump-only and bump-and-hole textures.

#### A.2.2 Material Models

Only the seal lip has been modeled in the three dimensional simulations. The same elastomeric material parameters that were used previously were again employed here. A deformed three dimensional mesh of the hole-bump texture is shown in Figure A.5.

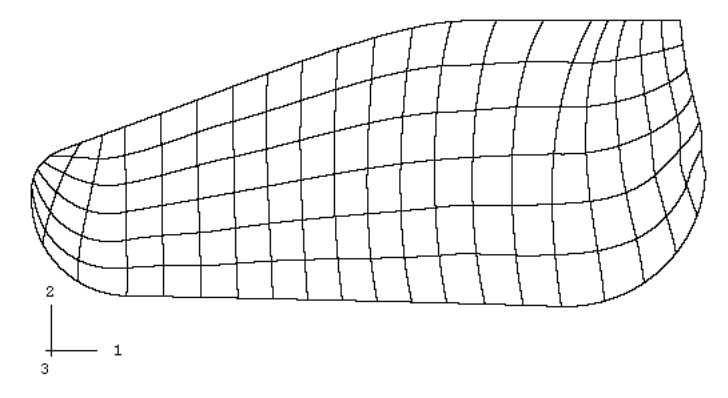


Figure A. 1: Deformed mesh of a seal that has been compressed under 2.2 kN.

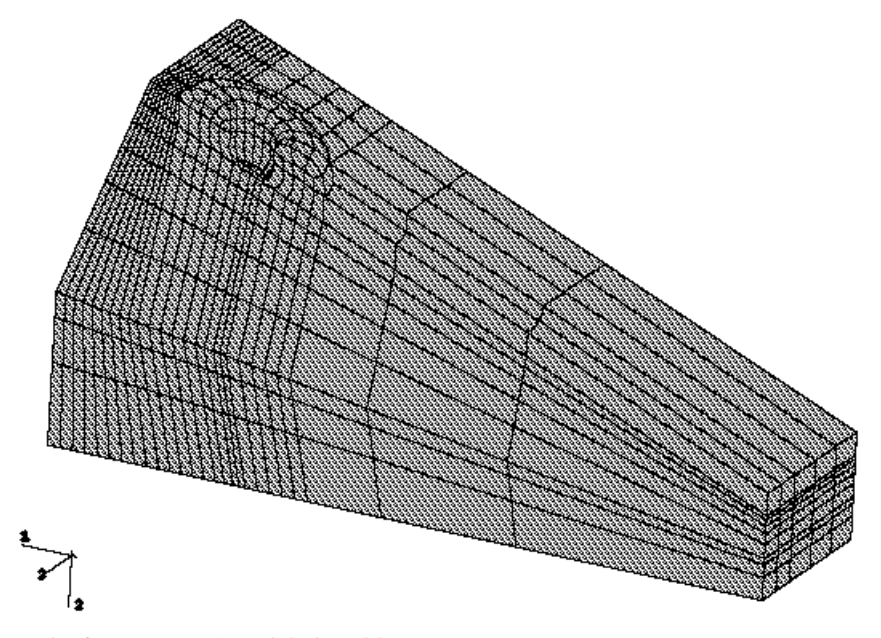


Figure A. 2: Portion of modeled seal lip.

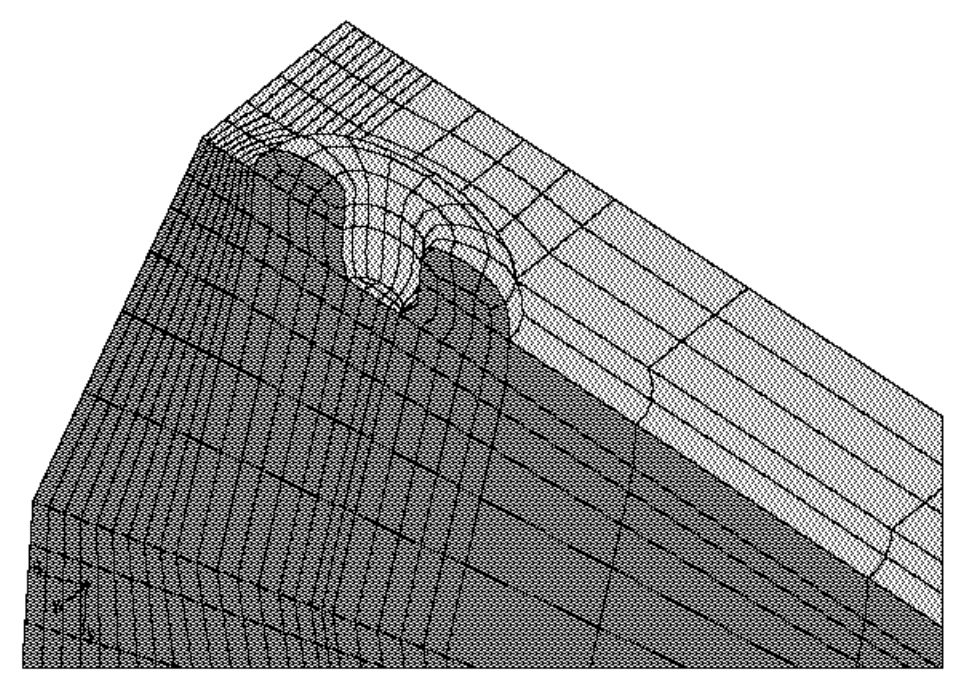


Figure A. 3: Detailed view of bump-and-hole texture.

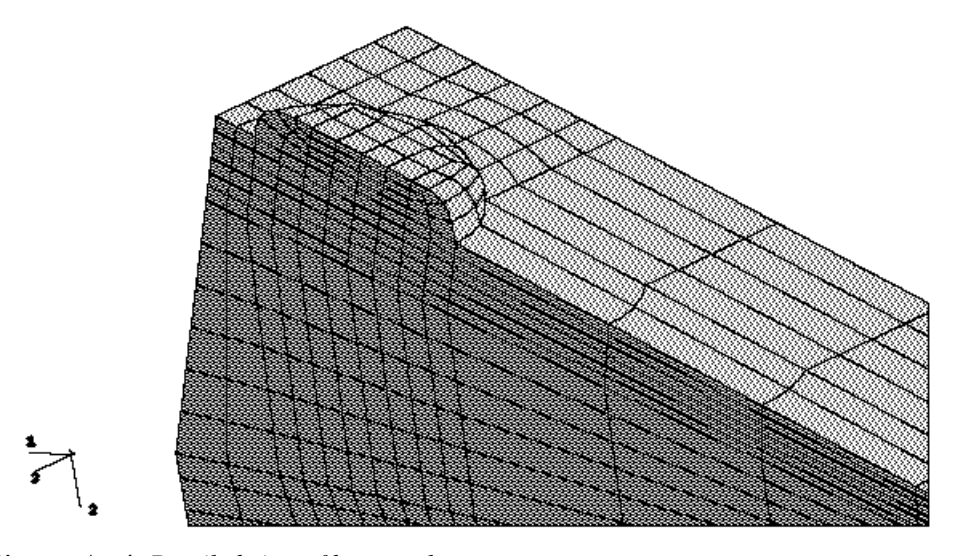


Figure A. 4: Detailed view of bump-only texture.

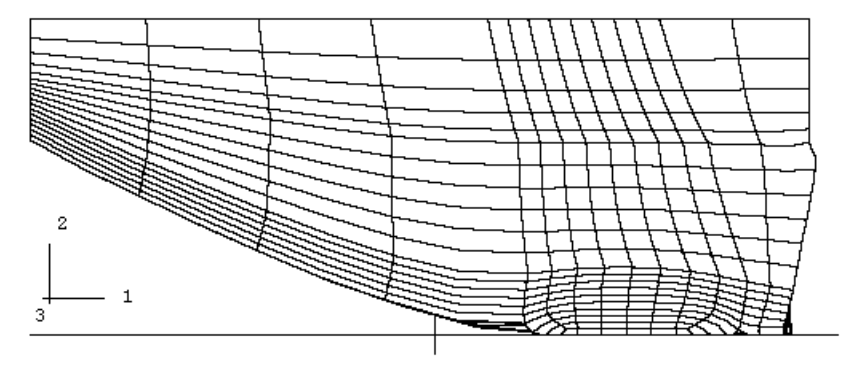


Figure A. texture.

5: Deformed three dimensional mesh of the bump-only texture.

#### **REFERENCES**

- [1] Lebeck, A. O., "Principles and Design of Mechanical Face Seals," John Wiley & Sons, Inc. (1991), pp. 3.
- [2] Hirabayashi, H., Kato, Y., and Ishiwata, H., 1967, "Excessive Abrasion of Mechanical Seals Caused by Salt Solutions," *Proceedings of the Third International Conference on Fluid Sealing*, BHRA, pp. B1-1–B1-15.
- [3] Golubiev, A., Gordeev, V., 1965, "Investigation of Wear Mechanical Seals in Liquids Containing Abrasive Particles," *Proceedings of the 7th International conference on Fluid Sealing*, Paper B3, pp. B3-23–B3-32.
- [4] Bratthäll, J., 1992, "Mechanical Seals for Abrasive and Clogging Media," *Proceedings of the13th International Conference on Fluid Sealing*, BRH Group, pp. 333-346.
- [5] Suh, N. P. (Ed), c1980, "Fundamentals of Tribology: proceeding of the International Conference on the Fundamentals of Tribology," MIT Press.
- [6] Poll, G., Gabelli, A., Binnington. P., Qu, J., 1992, "Dynamic Mapping of Rotary Lip Seal Lubricant Films by Fluorescent Image Processing," *Proceedings of the 13th Annual Conference on Fluid Sealing*, BHRA, pp. 55-77.
- [7] Tian, H., Saka, N., Suh, N. P., 1989, "Boundary Lubrication Studies on Undulated Titanium Surfaces", *Tribology Transactions*, Vol. 32, **3**, pp. 289-296.
- [8] Arruda, E.M., Boyce, M.C., "Three Dimensional Constitutive Model for the Large Stretch Behavior or Rubber Elastic Materials," *J. Mech. Physics of Solids*, 1993.